nanomaterials

MDPI

Article

Dual-Platform Evaluation of Charge-Modulated Betanin Delivery Using Cellular and Organismal Models

Eunhye Kim [1,2,†], Sunhee Yoon [1,2,†], Tae-Joon Jeon [1,2,3,*] and Sun Min Kim [1,2,4,*]

[1] Department of Biological Sciences and Bioengineering, Inha University, Incheon 22212, Republic of Korea; dsm5477@gmail.com (E.K.); yoonsh0912@inha.ac.kr (S.Y.)
[2] Biohybrid Systems Research Center (BSRC), Inha University, Incheon 22212, Republic of Korea
[3] Department of Biological Engineering, Inha University, Incheon 22212, Republic of Korea
[4] Department of Mechanical Engineering, Inha University, Incheon, 22212, Republic of Korea
* Correspondence: tjjeon@inha.ac.kr (T.-J.J.); sunmk@inha.ac.kr (S.M.K.)
† These authors contributed equally to this work.

Abstract

Betanin has potential for modulating lipid accumulation, but its biological activity depends on formulation and exposure conditions. We evaluated charge-modulated betanin liposomes in free fatty acid (FFA)-treated HepG2 cells and high-glucose-exposed *Caenorhabditis elegans*. Increasing DOTAP content from 0 to 30 mol% raised the zeta potential from −3.24 ± 0.12 to 31.09 ± 1.22 mV and the encapsulation efficiency from 35.21 ± 1.85% to 50.05 ± 1.70%. NBD-CL2 produced approximately 156-fold higher cell-associated fluorescence than NBD-CL0 in HepG2 cells, with higher fluorescence also observed descriptively in *C. elegans*. At the efficacy concentrations (25 μM betanin-equivalent in HepG2 cells and 50 μM in *C. elegans*), no apparent reduction in cell viability or survival was observed; pooled worm body-length measurements showed no overt change but did not support inference among independent exposure wells. In analyses accounting for experimental run, Bet-CL2 reduced Oil Red O intensity by 33.0% relative to the FFA-treated HepG2 group ($n = 4$ runs; Dunnett-adjusted $p = 0.0061$) and by 36.4% relative to the high-glucose *C. elegans* group ($n = 3$ runs; adjusted $p = 0.017$). These separate within-model results support attenuation of lipid accumulation in both models under the tested conditions, but do not establish cross-model statistical equivalence or superiority over free betanin or neutral liposomes. Carrier-associated fluorescence does not directly quantify betanin delivery. The dual-model approach supports complementary evaluation of carrier association and functional responses.

Keywords: betanin; surface charge modulation; HepG2; *C. elegans*; lipid accumulation; alternative metabolic model

Check for updates

Academic Editor: Stefano Leporatti

Received: 27 October 2026
Revised: 16 November 2026
Accepted: 16 November 2026
Published: 18 November 2026

Copyright: © 2026 by the authors. Licensee MDPI, Basel, Switzerland. This article is an open access article distributed under the terms and conditions of the Creative Commons Attribution (CC BY) license.

1. Introduction

Obesity is characterized by excessive lipid accumulation and dysregulated metabolic homeostasis and is a major risk factor for chronic metabolic diseases, including type 2 diabetes and non-alcoholic fatty liver disease (NAFLD) [1,2]. Although various pharmacological approaches have been developed to treat obesity and related metabolic disorders, adverse effects associated with some treatments, including cardiovascular complications and gastrointestinal disturbances, remain concerns during long-term use [2]. These limitations have stimulated interest in natural bioactive compounds with potentially favorable safety profiles and suitability for long-term metabolic management [3].

Betanin (betanidin 5-O-β-glucoside) is a major betalain pigment abundant in beetroot (Beta vulgaris) and has been reported to exhibit antioxidant, anti-inflammatory, and lipid

metabolism-modulating activities [4–7]. Its ability to mitigate oxidative stress and suppress lipid accumulation has attracted attention for its potential applications in metabolic disease management [5,8]. However, betanin exhibits limited stability under physiological conditions and is susceptible to changes in pH, oxidative conditions, and enzymatic degradation, which may compromise its biological efficacy [9–11]. These properties may limit effective delivery and diminish its biological activity at both the cellular and whole-organism levels.

Various delivery systems, including liposomes, have been investigated to address the stability and delivery limitations of betanin [9,10,12–14]. Previous studies have reported that liposomal encapsulation can improve storage stability, enhance betanin retention under gastrointestinal conditions, and preserve biological activity [9,15]. Cationic surface modification has also shown potential for enhancing interactions with biological interfaces [13,16]. Nevertheless, much of the existing research has focused on formulation stability, controlled release, or specific therapeutic applications. Although the biological interactions of cationic delivery systems have been extensively investigated at both the cellular and organismal levels, studies that integrate metabolic phenotypes across these levels remain relatively limited.

Cationic liposomes contain positively charged lipid components that can promote electrostatic interactions with negatively charged cell membranes and other biological interfaces, potentially enhancing membrane association and cellular internalization [17]. Cationic lipids such as DOTAP have therefore been widely used in lipid-based delivery systems to enhance cellular uptake and delivery efficiency [18,19]. Surface engineering through charge modulation may thus provide a strategy for regulating the biological responses to natural compound delivery systems. However, its implications for metabolic efficacy remain insufficiently explored using alternative metabolic models.

There is growing interest in alternative in vivo models that complement conventional mammalian models in metabolic research. *Caenorhabditis elegans* possesses conserved lipid metabolic pathways and is widely used to assess metabolic phenotypes at the whole-organism level [20–30]. Its short generation time and experimental tractability also support its use in evaluating biological responses to natural compounds and nanoparticle delivery systems [25–27,31]. Exposure in liquid culture provides a straightforward setting for comparing delivery-associated responses. Combining a HepG2 cellular steatosis model with a *C. elegans* alternative metabolic model may therefore enable an integrated assessment of the biological efficacy of charge-modulated delivery systems at the cellular and whole-organism levels.

In this study, DOTAP-containing cationic liposomes were employed as a tool for betanin delivery and surface charge modulation to compare charge-dependent uptake-associated behavior and lipid accumulation responses in HepG2 cells and *C. elegans* (Figure 1). Betanin-loaded cationic liposomes were prepared and characterized, and their uptake characteristics, safety, and efficacy in reducing lipid accumulation were evaluated using a dual-model metabolic platform comprising HepG2 cells and *C. elegans*. This platform was used to assess delivery-associated biological responses to betanin across cellular and whole-organism models. HepG2 cells were used here as a hepatocyte-like model in which free fatty acid exposure reproducibly induces intracellular lipid accumulation, and which is widely applied in studies of hepatic steatosis and non-alcoholic fatty liver disease, rather than as a cancer target. The study was therefore not designed to compare anticancer selectivity across tumor cell lines; the whole-organism *C. elegans* evaluation was included to provide complementary information on efficacy and tolerability in an intact animal that contains non-transformed tissues.

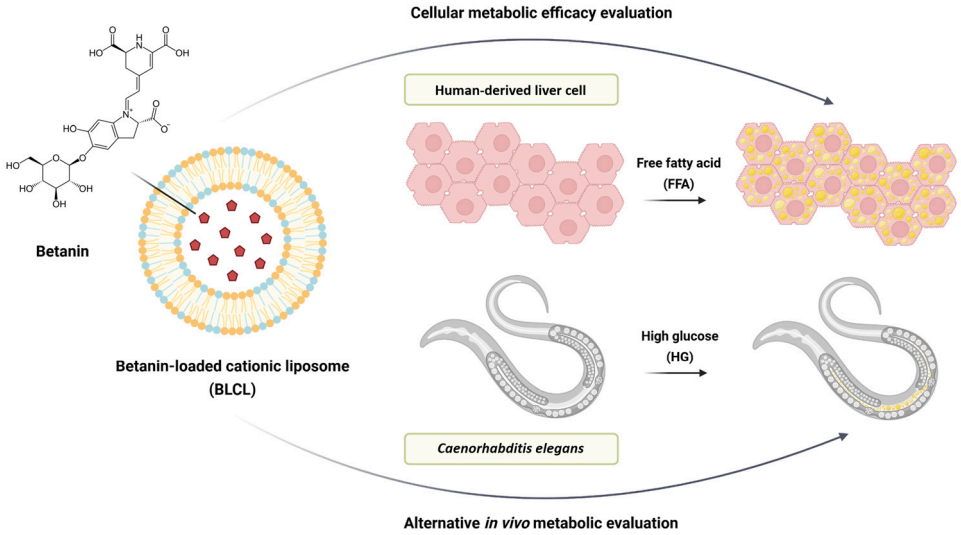


Figure 1. Schematic illustration of the dual-model evaluation strategy for charge-modulated betanin delivery. Betanin was encapsulated in liposomes with varying DOTAP contents (0–30 mol%) to prepare betanin-loaded cationic liposomes (BLCLs), which served as delivery tools for surface charge modulation. Within each model, all formulations were tested at an equivalent final betanin concentration: 25 μM for HepG2 cells and 50 μM for *C. elegans*. (**Top**) Cellular metabolic evaluation: A cellular steatosis model was established in human hepatocellular carcinoma-derived HepG2 cells by inducing intracellular lipid accumulation with BSA-conjugated free fatty acids (FFAs; 0.5 mM), comprising oleic acid and palmitic acid at a 2:1 ratio. For efficacy evaluation, cells were co-treated with FFAs and betanin formulations for 24 h. (**Bottom**) Whole-organism metabolic evaluation: A whole-organism lipid accumulation model was established by culturing synchronized L1-stage *C. elegans* N2 in liquid medium containing 50 mM glucose (high glucose, HG) for approximately 48 h until the L4 stage. The worms were then washed with M9 buffer and treated with betanin formulations for 24 h. Both models were evaluated for carrier-associated fluorescence, safety (HepG2 cell viability and *C. elegans* body length and survival), and lipid accumulation assessed by Oil Red O staining.

2. Materials and Methods

2.1. Preparation of Charge-Modulated Betanin Delivery Formulations

Betanin-loaded liposomes were prepared by mixing egg phosphatidylcholine (Egg PC; Avanti Polar Lipids, Alabaster, AL, USA; Cat. No. 840051) and cholesterol (Sigma-Aldrich, St. Louis, MO, USA; Cat. No. C8667) dissolved in chloroform (Sigma-Aldrich, St. Louis, MO, USA; Cat. No. 319988) at the specified molar ratios, with the total lipid concentration adjusted to 2 mg/mL. The lipid mixture was transferred to a 10 mL glass vial, and the solvent was evaporated under a stream of argon at room temperature to form a dry lipid film. The film was subsequently hydrated with betanin-containing phosphate-buffered saline (PBS, pH 7.4; SolBio, Suwon, Republic of Korea; Cat. No. PBS-001; betanin: Sigma-Aldrich, St. Louis, MO, USA; Cat. No. 901266) and vortexed for 2 min to form multilamellar vesicles. To obtain a uniform liposome dispersion, the suspension was extruded 21 times through a polycarbonate membrane (Whatman Nuclepore, Cytiva, Marlborough, MA, USA; Cat. No. 10417004) with a pore size of 200 nm. The cholesterol content was fixed at 15 mol%, while the proportion of the cationic lipid DOTAP (Avanti Polar Lipids; Cat. No. 890890) was varied at 0, 10, 20, and 30 mol%. Egg PC constituted the remaining lipid fraction. The resulting betanin-loaded cationic liposome (BLCL) formulations were designated Bet-CL0, Bet-CL1, Bet-CL2, and Bet-CL3, respectively, according to their DOTAP content (Table S1). Betanin encapsulation efficiency (EE) was determined after separating non-encapsulated betanin from the liposomal fraction, and was calculated as:

$$EE\ (\%) = [(W_{total} - W_{free})/W_{total}] \times 100 \quad (1)$$

where W_{total} is the total amount of betanin added during hydration of the lipid film and W_{free} is the amount of non-encapsulated betanin recovered in the filtrate. Non-encapsulated betanin was separated from the liposomal fraction using a centrifugal filter with a molecular weight cutoff of 100 kDa (Amicon Ultra-0.5, MilliporeSigma, Burlington, MA, USA; Cat. No. UFC5100BK). The betanin concentration in the filtrate was determined from its absorbance at 538 nm, measured with a microplate reader (Varioskan LUX, Thermo Fisher Scientific, Bothell, WA, USA), using a calibration curve prepared with betanin standards after correction for the PBS background, and W_{free} was calculated by multiplying this concentration by the collected filtrate volume.

2.2. Establishment of the HepG2 Lipid Accumulation Model and Treatment

The human hepatocellular carcinoma cell line HepG2 was purchased from the Korean Cell Line Bank (KCLB, Seoul, Republic of Korea). Cells were cultured in Dulbecco's modified Eagle's medium (DMEM; Gibco, Thermo Fisher Scientific, Waltham, MA, USA; Cat. No. 11995065) supplemented with 10% fetal bovine serum (FBS; Gibco, Thermo Fisher Scientific, Waltham, MA, USA; Cat. No. 10082147) and 1% penicillin–streptomycin (Gibco, Thermo Fisher Scientific, Waltham, MA, USA; Cat. No. 15140122) and maintained at 37 °C in an incubator with 5% CO_2. Lipid accumulation was induced using a free fatty acid (FFA) mixture comprising oleic acid (Sigma-Aldrich, St. Louis, MO, USA; Cat. No. O1008) and palmitic acid (Sigma-Aldrich, St. Louis, MO, USA; Cat. No. P0500) at a 2:1 ratio. HepG2 cells were seeded in 24-well plates at a density of 1×10^5 cells/well and cultured for 24 h. The cells were then exposed to BSA-conjugated FFAs (BSA: Sigma-Aldrich, St. Louis, MO, USA; Cat. No. A7030) at a final concentration of 0.5 mM for 24 h to establish the steatosis model [32,33]. To evaluate the anti-steatotic efficacy of the liposome formulations, cells were co-treated with the FFA mixture and liposome formulations for 24 h at a final betanin-equivalent concentration of 25 μM.

2.3. Establishment of the C. elegans Lipid Accumulation Model and Treatment

Wild-type *C. elegans* N2 and *Escherichia coli* OP50, used as the bacterial food source, were obtained from the Caenorhabditis Genetics Center (CGC, University of Minnesota, Minneapolis, MN, USA). Worms were maintained at 25 °C. To obtain synchronized L1 larvae, worms cultured on plates for 2 days were subjected to an egg preparation procedure according to a published protocol [34]. The collected eggs were incubated in M9 buffer for 24 h to obtain synchronized L1 larvae. To induce lipid accumulation, synchronized L1 larvae were cultured in 24-well plates containing liquid medium supplemented with 50 mM glucose (Sigma-Aldrich, St. Louis, MO, USA; Cat. No. G7021) and OP50 as a food source. Worms were grown for approximately 48 h until the L4 stage and then washed twice with M9 buffer. To evaluate the lipid accumulation-inhibitory efficacy of the liposome formulations, worms were distributed at 150–200 worms/well and treated with the formulations for approximately 24 h at a final betanin-equivalent concentration of 50 μM. FUdR (Sigma-Aldrich, St. Louis, MO, USA; Cat. No. F0503) was added at a final concentration of 100 μM during liposome treatment to suppress reproduction. The treatment concentrations of betanin were determined based on the distinct exposure characteristics of the two experimental models. For *C. elegans*, 50 μM was selected based on a previous study reporting the biological activity of red-beet-derived betalain pigments at this concentration [35]. Unlike *C. elegans*, in which compound exposure at the organismal level is influenced by ingestion, intestinal absorption, and tissue distribution, HepG2 cells are directly exposed to betanin-containing culture medium. Considering these differences in exposure conditions, a lower extracellular concentration of 25 μM was selected for HepG2 cells.

For the Oil Red O lipid accumulation assay, three independent experimental runs were performed on separate days, with all treatment conditions included in each run. One well per treatment condition was analyzed in each run, and five individual nematodes were randomly selected from each well. The five measurements were averaged to obtain a single well-level observation ($n = 3$ independent runs per treatment); data are reported as the mean ± SEM of these three well-level means. Sampling for the other *C. elegans* endpoints is described separately below and in the figure legends.

2.4. Assessment of Cytotoxicity and Organismal Toxicity

The cytotoxicity of betanin and betanin-loaded liposomes was evaluated using a Cell Counting Kit-8 (CCK-8; Dojindo Laboratories, Kumamoto, Japan; Cat. No. CK04) assay. HepG2 cells were seeded in 96-well plates at a density of 1×10^4 cells/well and cultured for 24 h. Betanin or betanin-loaded liposomes were diluted in cell culture medium and applied to the cells for 24 h. Following treatment, cells were washed twice with Dulbecco's phosphate-buffered saline (DPBS; SolBio, Suwon, Republic of Korea; Cat. No. DPB-001), and a mixture of cell culture medium and CCK-8 reagent was added. After incubation for 2 h, absorbance was measured using a microplate reader to determine cell viability. Toxicity in *C. elegans* was evaluated by measuring body length and survival. Worms grown to the L4 stage in liquid medium were treated with the liposome formulations for 24 h, after which body length was measured. Survival was also assessed in worms exposed to betanin or liposome formulations for approximately 10 days.

For each exposure concentration, three independent wells containing *C. elegans* were prepared and exposed under identical experimental conditions on the same day. Nematodes from the three wells were pooled, and 10–20 individuals were randomly selected for measurement. The results are presented as the mean ± SEM of the individual measurements. Because the nematodes were pooled before analysis, variability among the independent exposure wells could not be determined.

2.5. Analysis of Uptake-Associated Fluorescence

To evaluate uptake-associated behavior as a function of cationic surface charge, fluorescent liposomes were prepared by incorporating the fluorescent phospholipid analog 18:1 NBD PE (Avanti Polar Lipids, Alabaster, AL, USA; Cat. No. 810145) at 1 mol% of the total lipid composition. For fluorescence imaging in HepG2 cells, cells were seeded in 96-well plates at a density of 1×10^4 cells/well and cultured for 24 h. Fluorescent liposomes were diluted in cell culture medium and applied to the cells for 2 h. The cells were then washed twice with PBS and imaged using a fluorescence microscope (EVOS M7000, Thermo Fisher Scientific, Bothell, WA, USA). For quantitative analysis, liposome-derived NBD fluorescence associated with the cell surface or internalized by the cells was measured following treatment with NBD-labeled liposomes using a flow cytometer (Attune NxT Flow Cytometer, Thermo Fisher Scientific, Waltham, MA, USA). The same fluorescent liposomes were used to assess whole-organism uptake-associated fluorescence in *C. elegans*. L4-stage worms were placed in 24-well plates and exposed to fluorescent liposomes in liquid medium for 6 h. Following treatment, worms were washed twice with M9 buffer and imaged using a fluorescence microscope. Fluorescence intensity was quantified using ImageJ software (version 1.54g, National Institutes of Health, Bethesda, MD, USA).

2.6. Visualization of Lipid Accumulation by Oil Red O Staining

Oil Red O staining was performed to visualize lipid accumulation in HepG2 cells. The working solution was prepared by mixing distilled water and a 0.5% Oil Red O (Sigma-Aldrich, St. Louis, MO, USA; Cat. No. O0625) stock solution at a 4:6 ratio. Cells were

fixed with 4% paraformaldehyde (SolMate, GeneAll Biotechnology, Seoul, Republic of Korea) and stained with the Oil Red O working solution for 30 min at room temperature. Excess staining solution was removed by washing, and images were acquired using a light microscope (ICX41, Sunny Optical Technology, Ningbo, China). Lipid accumulation in *C. elegans* was assessed using a similar Oil Red O staining procedure. Stained worms were examined and imaged using a light microscope.

2.7. Statistical Analysis

Quantitative data are presented as the mean ± standard error of the mean (SEM), unless otherwise specified in the corresponding figure legends. For physicochemical characterization, independently prepared liposome formulations were used as experimental replicates. For cell-based assays, measurements were obtained from independently treated wells or samples, as specified in the corresponding figure legends. For *C. elegans* experiments, the experimental unit and sampling strategy were defined according to the assay. In experiments involving pooled nematodes, individuals from three independently treated wells were combined, and 10–20 nematodes were randomly selected for analysis, depending on the experiment. These measurements were used to describe inter-individual variability and were not treated as independent experimental replicates.

For the *C. elegans* lipid accumulation assay, three independent experimental runs were performed, with all treatment conditions included in each run. One well per treatment condition was analyzed in each run, and five nematodes were randomly selected from each well. The measurements from the five nematodes were averaged to obtain a single well-level mean, which was treated as an independent experimental observation ($n = 3$ per treatment). The results are expressed as the mean ± SEM of the three well-level means.

All statistical analyses were performed using jamovi (version 2.7.41). Statistical differences among three or more independent groups were assessed using ordinary one-way analysis of variance (ANOVA) followed by Tukey's multiple comparisons test or Welch's one-way ANOVA followed by Games–Howell's post hoc test, depending on the variance structure of the data. For the Oil Red O lipid accumulation assays, which comprised four independent experimental runs in HepG2 cells and three independent experimental runs in *C. elegans*, each containing all treatment conditions, treatment effects were evaluated using a block ANOVA, with treatment as a fixed factor and experimental run as a blocking factor to account for run-to-run variability. Dunnett's multiple comparisons test was subsequently performed using the FFA-treated group (HepG2 cells) or the high-glucose group (*C. elegans*) as the reference. In both assays, run-level values were normalized to the overall mean of the control group, calculated from the run-level control values; because a single common factor was applied to all values, this normalization does not affect the F statistics or *p*-values. Relative reductions were calculated as 100 × (mean of the induction control − mean of the treatment group)/mean of the induction control. Confidence intervals are Dunnett-adjusted 95% simultaneous intervals for mean differences on the normalized scale. Normality of residuals was assessed using the Shapiro–Wilk test (HepG2 cells, $p = 0.19$; *C. elegans*, $p = 0.96$), and homogeneity of variance using the Brown–Forsythe test ($p = 0.48$ and $p = 0.60$, respectively). Comparisons between two independent groups were performed using an unpaired two-tailed Student's *t*-test, where appropriate. Statistical significance was defined as $p < 0.05$, with adjusted *p*-values used for multiple comparisons. The blocked analysis was chosen to reflect the inclusion of all treatments within each run, rather than on the basis of the significance of the block effect. The additive model included treatment and run effects, without a treatment-by-run interaction, because only one observation was obtained per treatment-by-run combination and the interaction could therefore not be estimated separately from residual error. The experimental-run effect was statistically

significant in both lipid accumulation assays (HepG2 cells, $F(3,12) = 11.97$, $p = 0.0006$; *C. elegans*, $F(2,8) = 5.46$, $p = 0.032$). Unblocked one-way ANOVA followed by Tukey's test gave $p = 0.22$ for HepG2 cells and $p = 0.115$ for *C. elegans* for Bet-CL2 versus the respective induction control. These sensitivity analyses differ from the primary analyses in both the treatment of run effects and the multiple-comparison procedure. The reported partial η^2 values refer to the omnibus treatment effect. Analyses were conducted separately for each model; no between-model treatment-effect or equivalence test was performed.

3. Results and Discussion

3.1. Physicochemical Characterization of Charge-Modulated Betanin Formulations

To establish a physicochemical basis for interpreting the biological responses observed in the cellular and *C. elegans* models, liposome particle size, size distribution, surface charge, and betanin encapsulation efficiency were evaluated as a function of DOTAP content (Figure 2 and Table S1). Incorporation of DOTAP significantly reduced the mean particle diameter from 176.30 ± 1.33 nm for Bet-CL0 to 159.07–162.63 nm for Bet-CL1–3, although further increases in DOTAP content produced only minor additional reductions in particle size (Figure 2A). All formulations exhibited polydispersity index (PDI) values ≤ 0.15, with a significant reduction observed only for Bet-CL3 (Figure S1). The most pronounced change was observed in zeta potential, which increased from −3.24 ± 0.12 mV for Bet-CL0 to 15.14 ± 0.67, 27.88 ± 1.05, and 31.09 ± 1.22 mV for Bet-CL1, Bet-CL2, and Bet-CL3, respectively (Figure 2B). These results demonstrate effective modulation of liposome surface charge through adjustment of DOTAP content and provide a physicochemical basis for interpreting potential electrostatic interactions with biological interfaces in HepG2 cells and *C. elegans*.

Encapsulation efficiency did not differ significantly between Bet-CL0 (35.21 ± 1.85%) and Bet-CL1 (37.20 ± 1.99%), whereas significant increases were observed for Bet-CL2 (42.74 ± 1.53%) and Bet-CL3 (50.05 ± 1.70%) compared with Bet-CL0 (mean ± SEM, $n = 10$; Figure 2C). In contrast, liposomes containing the anionic lipid DOPG exhibited an encapsulation efficiency of 35.80 ± 2.11%, significantly lower than that of the DOTAP-containing liposomes (52.35 ± 3.62%; $n = 3$) (Figure 2D). This finding suggests that betanin retention may be influenced by the polarity of the incorporated charged lipid rather than simply by its presence. Specifically, betanin carries carboxyl groups derived from its betalamic acid moiety, and these groups are largely deprotonated at neutral pH. The net negative charge of betanin under the hydration conditions used here (PBS, pH 7.4) therefore arises from the ionization state of the individual betanin molecule, and not from interactions between betanin molecules. Electrostatic attraction between the anionic carboxylate groups of betanin and the cationic quaternary ammonium headgroup of DOTAP is consequently expected to favor betanin retention in the liposomal phase, whereas the anionic headgroup of DOPG would be expected to repel betanin electrostatically. This interpretation is consistent with the lower encapsulation efficiency measured for the DOPG-containing formulation (Figure 2D) [36,37].

Overall, these physicochemical properties did not change in a simple linear manner with increasing DOTAP content. Moreover, excessive positive surface charge can promote strong interactions with cell membranes and induce cytotoxicity; thus, enhanced physicochemical characteristics do not necessarily translate into optimal biological performance [38]. We therefore investigated whether surface charge modulation could enhance biological association within a cytocompatibility range. It should also be noted that a higher encapsulation efficiency does not in itself demonstrate greater formulation stability or more effective release of betanin under biological conditions. The zeta potential and encapsulation efficiency

data in Figure 2 are therefore interpreted here as the physicochemical basis for electrostatic interaction with biological interfaces, rather than as direct evidence of improved delivery.

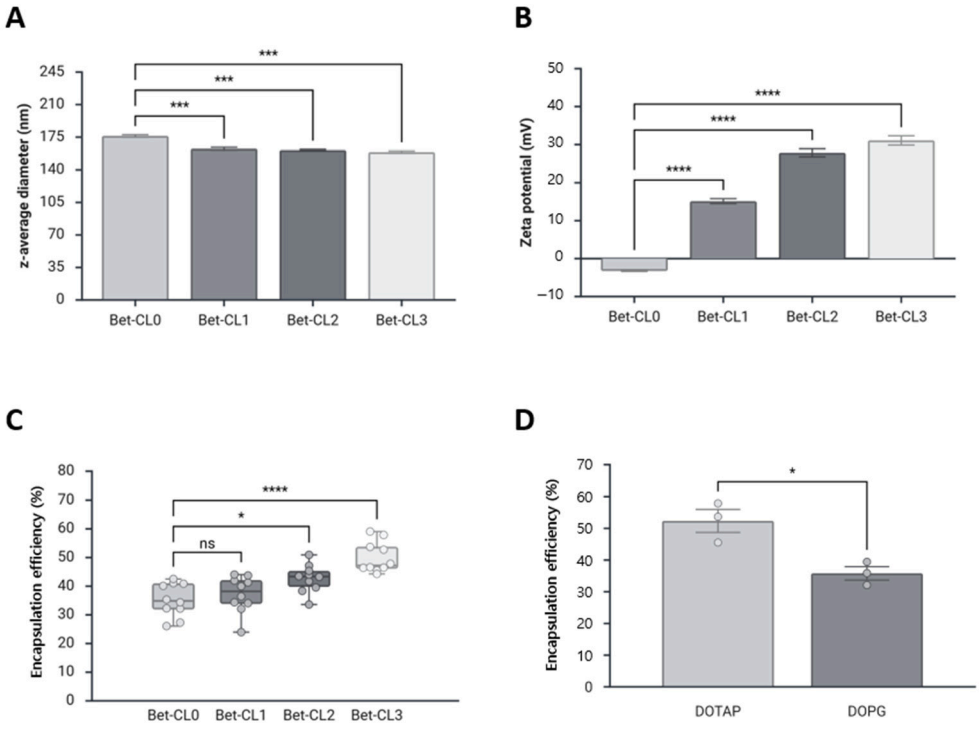


Figure 2. Physicochemical characterization of charge-modulated betanin formulations. (**A**) Mean particle diameter of betanin-loaded liposomes as a function of DOTAP content. (**B**) Zeta potential of betanin-loaded liposomes as a function of DOTAP content. (**C**) Betanin encapsulation efficiency as a function of DOTAP content. (**D**) Comparison of betanin encapsulation efficiency between cationic (DOTAP-containing) and anionic (DOPG-containing) liposomes. Data in (**A**,**B**,**D**) are presented as mean ± standard error of the mean (SEM) from three independent liposome preparations ($n = 3$ per group). Data in (**C**) are presented as box-and-whisker plots based on ten independent liposome preparations ($n = 10$ per group), with boxes representing the interquartile range (25th–75th percentiles), horizontal lines indicating the median, and whiskers extending from the minimum to the maximum values. Mean ± SEM values for (**C**) reported in the main text were calculated from the same ten preparations. Statistical significance was assessed using one-way analysis of variance (ANOVA) followed by Tukey's multiple comparisons test for (**A**–**C**), and an unpaired two-tailed Student's *t*-test for (**D**). ns, not significant ($p \geq 0.05$); * $p < 0.05$; *** $p < 0.001$; **** $p < 0.0001$.

3.2. Assessment of Betanin Biocompatibility and Establishment of Cellular and Whole-Organism Lipid Accumulation Models

Before evaluating the efficacy of betanin-loaded cationic liposomes (BLCLs) in reducing lipid accumulation, we assessed the toxicity of free betanin and verified the establishment of lipid accumulation models in HepG2 cells and *C. elegans* (Figure 3).

HepG2 cells treated with free betanin at concentrations of 10–1000 μM for 24 h maintained high viability across the tested concentration range, with no apparent concentration-dependent decline (Figure 3A). These findings indicate that the betanin concentrations used in subsequent efficacy experiments were within a range that did not induce overt cytotoxicity.

Similarly, betanin treatment did not cause apparent growth inhibition or reduced survival in *C. elegans*. Betanin-exposed worms developed normally to the L4 stage, and neither body length nor survival over 10 days showed a clear decline with increasing betanin concentration (Figure 3B,C). Together, these cellular and whole-organism findings

provide a basis for interpreting subsequent reductions in lipid accumulation in relation to the metabolic effects of betanin or its formulations, while helping to distinguish these responses from nonspecific cytotoxicity or growth inhibition.

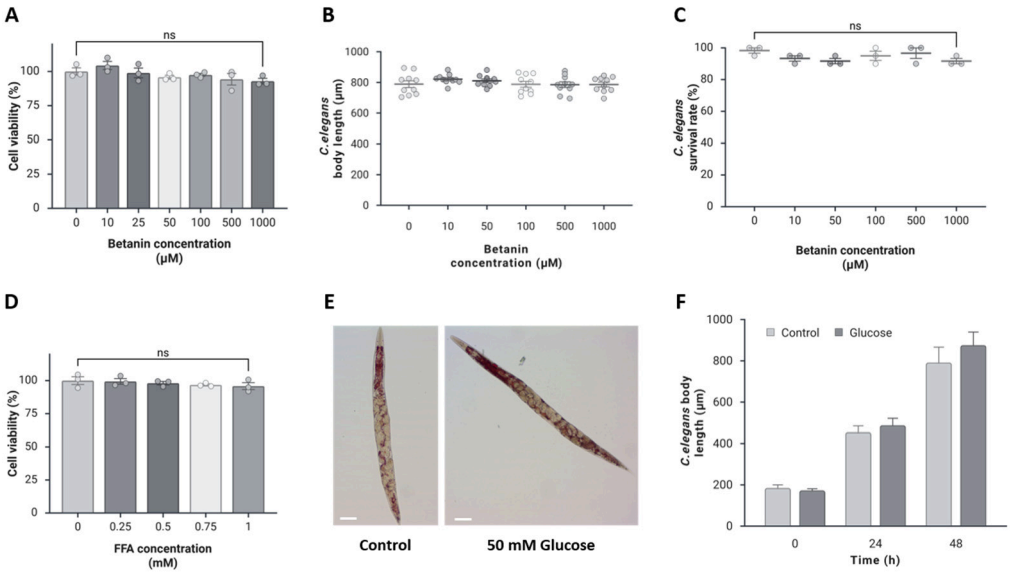


Figure 3. Toxicity assessment and establishment of lipid accumulation models in HepG2 cells and *C. elegans*. (**A**) Viability of HepG2 cells treated with various concentrations of betanin for 24 h ($n = 3$ wells per condition). (**B**) Body length of *C. elegans* exposed to various concentrations of betanin. Nematodes from three independently treated wells per concentration were pooled, and 10 individuals were randomly selected for measurement ($n = 10$ worms per group). (**C**) Survival of *C. elegans* cultured in betanin-containing medium for 10 days ($n = 3$ wells per condition). (**D**) Viability of HepG2 cells following treatment with various concentrations of free fatty acids (FFAs) ($n = 3$ wells per condition). (**E**) Representative Oil Red O-stained images of *C. elegans* cultured under control conditions or in the presence of 50 mM glucose for 48 h. Scale bars = 100 μm. (**F**) Body length of *C. elegans* cultured under control and 50 mM glucose conditions at 0, 24, and 48 h. At each time point, nematodes from three independently treated wells per group were pooled, and 20 individuals were randomly selected for body-length measurement ($n = 20$ worms per group per time point). Data in (**A**–**D**,**F**) are presented as mean ± standard error of the mean (SEM). For (**B**,**F**), SEM represents variability among individual nematodes within pooled samples rather than variability among independent wells. Statistical significance was assessed using one-way analysis of variance (ANOVA) followed by Tukey's multiple comparisons test for (**A**,**C**,**D**). ns, not significant ($p \geq 0.05$).

Lipid accumulation models were subsequently established in HepG2 cells and *C. elegans* for efficacy evaluation. In HepG2 cells, the effects of FFAs on cell viability were first examined over a concentration range of 0–1 mM (Figure 3D). At 0.5 mM FFA, the concentration selected for subsequent induction of lipid accumulation, cell viability remained high, with no apparent reduction relative to the control group. Because excessive FFA exposure can induce lipotoxicity and cell death, it is important to identify conditions that induce lipid accumulation without overt cytotoxicity. Accordingly, 0.5 mM FFA was selected for the cellular model used to evaluate the efficacy of betanin formulations in reducing lipid accumulation. FFA-induced lipid accumulation was subsequently confirmed by Oil Red O staining in the efficacy experiments.

To establish the whole-organism lipid accumulation model, *C. elegans* was cultured in the presence of 50 mM glucose. Oil Red O staining was performed to verify whether high-glucose exposure induced a lipid accumulation phenotype. Glucose-treated worms exhibited more intense staining than control worms (Figure 3E), providing visual evidence of increased neutral lipid accumulation under these conditions. This finding is consistent

with previous reports that glucose supplementation increases triglyceride and neutral lipid accumulation in *C. elegans* [39–41].

Physiological responses to high-glucose exposure were further examined by measuring body length (Figure 3F). Body length increased over time in both the control and glucose-treated groups, with the glucose-treated group showing slightly greater mean body lengths at 24 and 48 h. However, because no between-group statistical significance is reported in Figure 3F, this observation should be interpreted as a trend in organismal growth under glucose-rich nutritional conditions rather than as a statistically significant increase in body size induced by high glucose. Moreover, increased body length is not a direct indicator of lipid accumulation but may represent an additional physiological phenotype reflecting the effects of the glucose-rich environment on organismal growth and energy metabolism.

Overall, the increased Oil Red O staining in Figure 3E directly visualizes the lipid accumulation phenotype induced under the high-glucose conditions used in this study, whereas the body-length changes in Figure 3F provide complementary information on organismal physiological responses to the same environment. The 50 mM glucose condition was therefore used to establish the *C. elegans* whole-organism lipid accumulation model for subsequent evaluation of the lipid-lowering efficacy of betanin and betanin-loaded liposomes. To further verify that both models could detect changes in lipid accumulation in response to betanin, free betanin was tested at different concentrations. In HepG2 cells, betanin treatment tended to reduce lipid accumulation compared with the FFA-only group, with the lowest mean values at 100–200 μM, whereas in *C. elegans*, lipid accumulation generally decreased with increasing betanin concentration (Figure S2).

3.3. Enhanced Biological Association Following Cationic Surface Modification and the Efficacy–Cytotoxicity Trade-Off

We investigated whether the DOTAP-induced changes in physicochemical properties translated into differences in interactions with biological interfaces. NBD-labeled liposomes were used to compare the fluorescence association of neutral and cationic formulations with HepG2 cells (Figure 4A,B).

Only a weak fluorescence signal was observed following treatment with the neutral formulation NBD-CL0, whereas the DOTAP-containing formulation NBD-CL2 produced a markedly stronger signal. Flow cytometric analysis showed relative mean fluorescence intensity (MFI) values of 1.00 ± 0.01, 1.21 ± 0.01, and 188.35 ± 8.93 for the control, NBD-CL0, and NBD-CL2 groups, respectively (Figure 4B). Thus, under the experimental conditions used, cell-associated fluorescence was approximately 156-fold higher for NBD-CL2 than for NBD-CL0. NBD-CL2 exhibited significantly higher fluorescence than the control group ($p < 0.01$), whereas NBD-CL0 produced a signal comparable to that of the control. These findings indicate that the marked increase in cell-associated fluorescence was associated with the DOTAP-containing cationic surface rather than with liposome exposure alone.

This difference can be interpreted in relation to the surface charge changes shown in Figure 2. The CL0 formulation exhibited a near-neutral surface charge, whereas the CL2 composition yielded a positive zeta potential of approximately +28 mV. Cationic liposomes can interact electrostatically with negatively charged phospholipids, proteoglycans, and other cell-surface components, potentially enhancing membrane association and subsequent endocytic processing [17,19,42]. The increased fluorescence observed here therefore suggests that cationic surface engineering enhanced interactions with the biological interface. However, because NBD fluorescence reflects a signal associated with liposomal lipids, these findings alone do not directly demonstrate the internalization of intact liposomes or an increase in intracellular betanin concentration. Accordingly, the results were interpreted specifically as cell-associated or uptake-associated fluorescence.

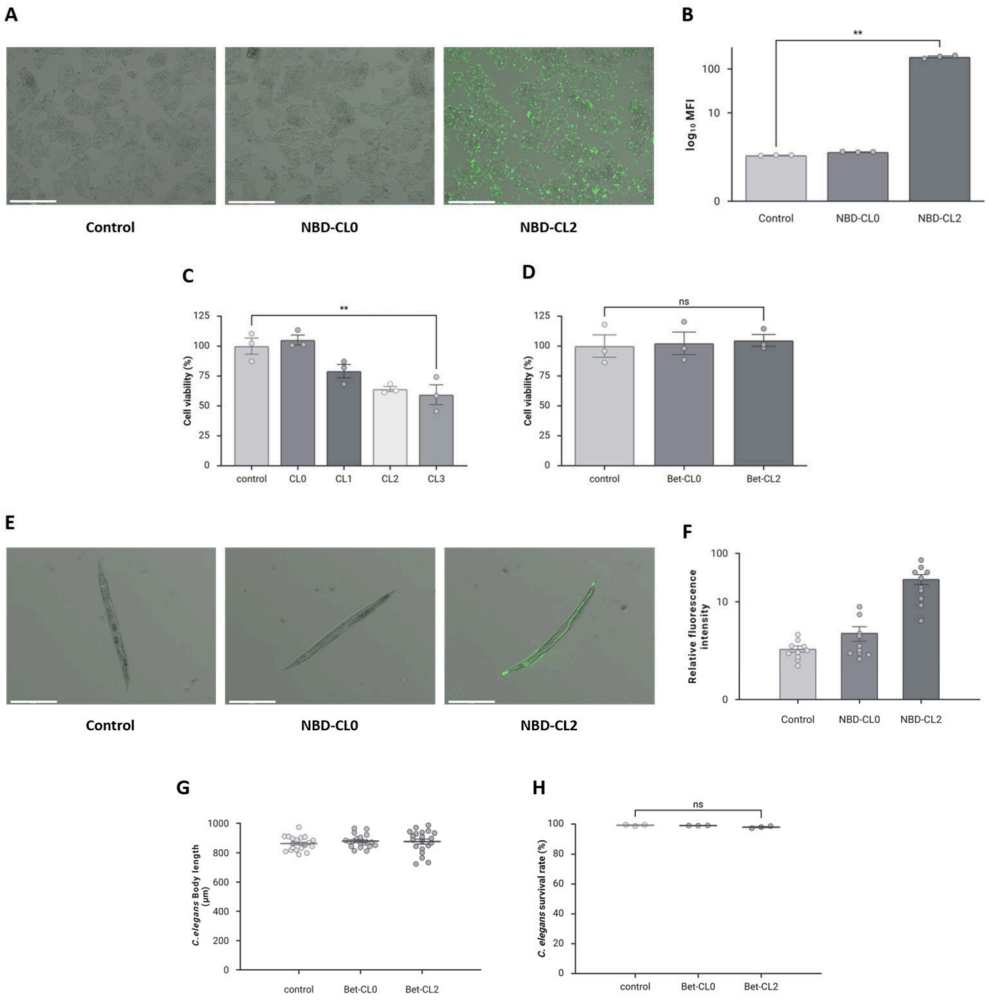


Figure 4. Evaluation of uptake-associated behavior and safety of cationic liposomes in HepG2 cells and *C. elegans*. (**A**) Representative fluorescence images of HepG2 cells treated with NBD-labeled liposomes with different DOTAP contents. Increased fluorescence intensity was observed following treatment with DOTAP-containing liposomes. Scale bar = 275 μm. (**B**) Quantification of cell-associated fluorescence intensity in HepG2 cells treated with NBD-labeled liposomes with different DOTAP contents. (**C**) Viability of HepG2 cells treated with liposomes with varying DOTAP contents. (**D**) Viability of HepG2 cells treated with betanin-loaded liposomes at the concentration used for efficacy evaluation (25 μM betanin). (**E**) Representative whole-organism fluorescence images of *C. elegans* following treatment with NBD-labeled liposomes. Increased uptake-associated fluorescence was observed following treatment with DOTAP-containing liposomes. Scale bar = 275 μm. (**F**) ImageJ-based quantification of fluorescence intensity in *C. elegans*, with 10 individual nematodes analyzed per treatment group (n = 10 worms per group). (**G**) Body length of *C. elegans* following treatment with betanin-loaded liposomes, with 20 individual nematodes analyzed per treatment group (n = 20 worms per group). (**H**) Survival of *C. elegans* following treatment with betanin-loaded liposomes. Quantitative data are presented as mean ± standard error of the mean (SEM). For (**F**,**G**), SEM represents inter-individual variability rather than variability among independent experimental replicates. Statistical significance was assessed using Welch's one-way ANOVA followed by Games–Howell's multiple comparisons test for (**B**), and ordinary one-way ANOVA followed by Tukey's multiple comparisons test for (**C**,**D**,**H**). ns, not significant ($p \geq 0.05$); ** $p < 0.01$. For (**B**–**D**), n = 3 independent cell-culture replicates per group; for (H), n = 3 plates per group.

An important consideration alongside enhanced biological association is the cytotoxicity of blank liposomes. To assess the effects of increasing DOTAP content on carrier toxicity, HepG2 cell viability was evaluated following treatment with blank liposomes containing no betanin (Figure 4C). Relatively high liposome exposure was used to examine the potential

cytotoxicity of the carriers themselves, with cell culture medium and liposome suspension mixed at an approximately 1:1 ratio. Cell viability tended to decrease with increasing DOTAP content. CL2 produced a clear reduction in viability relative to the control and CL0 groups, while CL3, which contained the highest proportion of DOTAP, yielded the lowest viability. In the CL3-treated group, viability was approximately 40.6% lower than that in the control group. These results indicate that, although increasing positive surface charge can enhance cellular association, it may also increase the risk of cytotoxicity under high-exposure conditions through stronger interactions with cell membranes.

The safety of betanin-loaded formulations was assessed separately under the conditions used for anti-steatotic efficacy evaluation (Figure 4D). In this experiment, formulations were administered at an equivalent final betanin concentration of 25 μM rather than at equal liposome suspension volumes. Consequently, total liposome and DOTAP exposure was substantially lower than under the high-exposure conditions used for the blank liposome assay in Figure 4C. Cell viability remained high in the control, Bet-CL0, and Bet-CL2 groups, with no apparent reduction following Bet-CL2 treatment (Figure 4D). The lower viability observed with blank CL2 in Figure 4C, compared with the absence of apparent toxicity following Bet-CL2 treatment in Figure 4D, should therefore not be attributed to a cytoprotective effect of betanin, because the two experiments involved different liposome and DOTAP exposure levels. Instead, these findings indicate that the biological safety of cationic formulations can depend strongly on the administered dose and exposure conditions, in addition to surface charge. Thus, although Bet-CL3 exhibited the highest zeta potential and encapsulation efficiency in Figure 2, selecting the formulation with the greatest positive charge alone was not considered appropriate given the cytotoxicity risk associated with higher DOTAP content. Bet-CL2 was selected for subsequent efficacy evaluation because it combined markedly increased uptake-associated fluorescence with high cell viability at the concentration used for efficacy testing, providing a balance between biological association and cytocompatibility. Because the blank liposome assay in Figure 4C and the efficacy-concentration assay in Figure 4D were performed at different carrier exposure levels, the viability data in Figure 4C provide the reference for carrier-only toxicity. At the betanin-equivalent concentration used for efficacy evaluation, neither Bet-CL0 nor Bet-CL2 produced an apparent reduction in viability. These results concern betanin-loaded formulations and do not exclude a contribution of the blank carrier to the lipid accumulation response. Bet-CL3 was not advanced to the efficacy evaluation because the corresponding blank formulation CL3 produced the largest reduction in viability under high-exposure conditions, approximately 40.6% below the control group, supporting the decision to advance Bet-CL2. However, Bet-CL3 was not tested at the efficacy exposure level, so these data do not establish that Bet-CL2 is safer or more effective than Bet-CL3 at matched exposure.

Uptake-associated fluorescence was also evaluated in *C. elegans*. NBD-CL2-treated worms exhibited a stronger fluorescence signal than NBD-CL0-treated worms (Figure 4E), and ImageJ-based quantification likewise showed markedly higher fluorescence intensity in the NBD-CL2 group (Figure 4F). The mean fluorescence intensity of the NBD-CL0 group was comparable to that of the control group, whereas the NBD-CL2 group showed a markedly higher mean intensity. Because nematodes from the three independently treated wells were pooled before imaging, these measurements describe inter-individual variability and were not subjected to statistical testing. Consistent with the observations in HepG2 cells, these findings suggest greater biological association or retention of the cationic formulation than of the neutral formulation at the whole-organism level. However, fluorescence in *C. elegans* cannot be attributed exclusively to tissue uptake. Following oral exposure, retention within the intestinal lumen, association with the intestinal surface, and tissue-associated fluorescence may all contribute to the measured signal. These results therefore do not

constitute direct evidence of enhanced systemic absorption or biodistribution and were interpreted as whole-organism uptake-associated fluorescence.

At the concentrations used for efficacy evaluation, Bet-CL treatment was not associated with changes in body length or with reductions in survival (Figure 4G,H). Both Bet-CL0- and Bet-CL2-treated worms maintained body lengths comparable to those of the control group and exhibited high survival. These findings indicate that the Bet-CL2 treatment conditions used in the efficacy experiments did not cause overt adverse effects on *C. elegans* growth or survival.

Taken together, DOTAP-mediated cationic surface modification increased formulation-associated fluorescence in both HepG2 cells and *C. elegans*. However, high exposure to cationic lipids was associated with a risk of cytotoxicity in HepG2 cells, highlighting the importance of balancing biological association and safety when selecting a formulation. From this perspective, Bet-CL2 exhibited enhanced uptake-associated behavior without overt toxicity at either the cellular or whole-organism level under the conditions used for efficacy testing and was therefore selected for subsequent evaluation of lipid accumulation responses.

3.4. Effects of Betanin-Loaded Cationic Liposomes on Lipid Accumulation in the Cellular and Whole-Organism Models

Oil Red O staining was performed in the HepG2 and *C. elegans* lipid accumulation models to evaluate the efficacy of charge-modulated betanin delivery in reducing lipid accumulation (Figure 5). Because the preceding fluorescence analyses showed enhanced uptake-associated behavior of the cationic formulation in both models, we investigated whether this increased biological association translated into changes in the lipid accumulation phenotype.

In the HepG2 steatosis model, treatment with 0.5 mM FFA increased intracellular lipid accumulation, whereas free betanin treatment produced a modest reduction in lipid staining intensity (Figure 5A). The neutral formulation Bet-CL0 showed a similar tendency, while the DOTAP-containing formulation Bet-CL2 exhibited a more pronounced reduction. Quantitative analysis showed that relative Oil Red O intensity increased to approximately 20 in the FFA-treated group. Mean staining intensity progressively decreased across the free betanin, Bet-CL0, and Bet-CL2 groups, with the lowest mean value observed for Bet-CL2 (Figure 5B). Based on the plotted mean values, Oil Red O intensity in the Bet-CL2 group was approximately 33% below that in the FFA-treated group, and this reduction was statistically significant (block ANOVA, $F(4,12) = 40.38$, $p < 0.0001$, partial $\eta^2 = 0.93$; mean difference, 6.83 relative intensity units; Dunnett-adjusted $p = 0.0061$; 95% simultaneous CI, 2.03 to 11.64). Free betanin and Bet-CL0 also lowered the mean intensity relative to the FFA-treated group, by approximately 15% and 17%, respectively, but neither reduction reached statistical significance (Dunnett-adjusted $p = 0.24$ and $p = 0.16$).

The fluorescence and lipid accumulation results describe different endpoints and comparisons. The approximately 156-fold fluorescence difference compares NBD-CL2 with NBD-CL0, whereas the approximately 33% reduction in Oil Red O intensity compares Bet-CL2 with the FFA-treated group. The assays also used different labels and exposure schedules. These numerical magnitudes therefore cannot establish proportionality, or its absence, between carrier association and the metabolic response.

Carrier association, intracellular cargo release, subcellular localization, betanin stability, metabolic processing, and signaling could each influence the final phenotype. These processes were not measured directly here. In particular, NBD fluorescence reports labeled liposomal lipids rather than intracellular betanin concentration. Thus, the higher fluorescence in Figure 4 and the lower Oil Red O intensity in Figure 5 are complementary

observations; they do not establish a causal or quantitative relationship between betanin delivery and lipid accumulation.

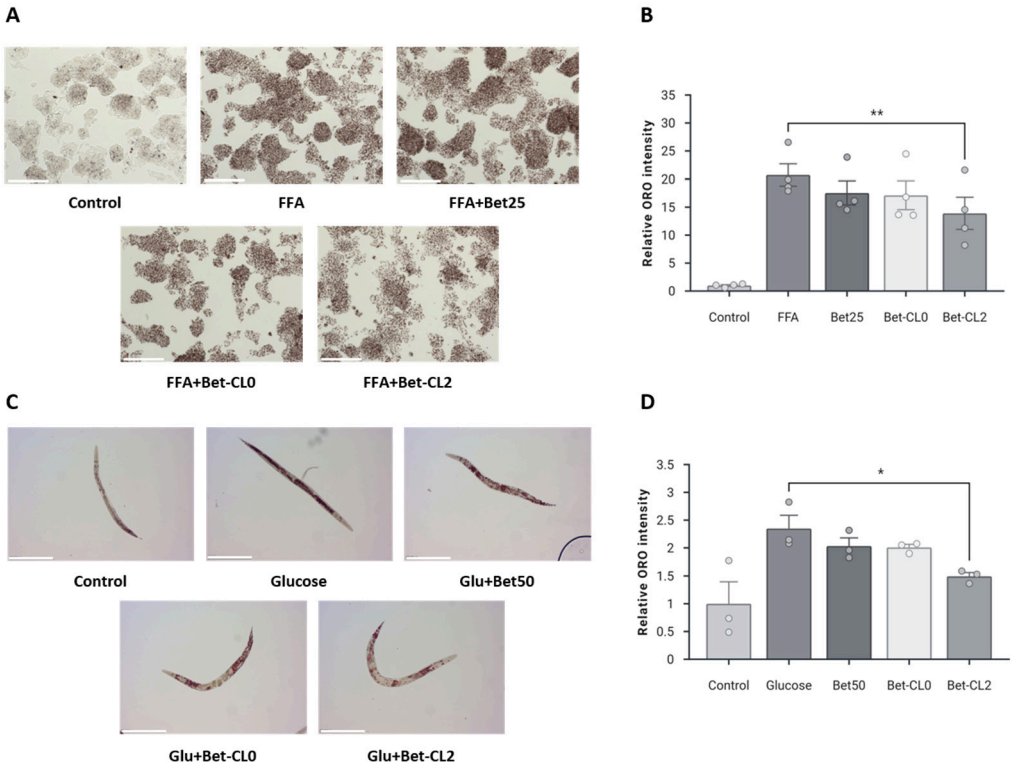


Figure 5. Effects of betanin-loaded cationic liposomes on lipid accumulation in the cellular and whole-organism models. (**A**) Representative Oil Red O-stained images of HepG2 cells co-treated with 0.5 mM free fatty acids (FFAs) and free betanin or betanin-loaded liposomes (25 µM betanin) for 24 h. Scale bar = 275 µm. (**B**) ImageJ-based quantification of intracellular lipid accumulation in HepG2 cells. Four independent experimental runs were performed, with all treatment conditions included in each run (n = 4 independent runs per group). (**C**) Representative Oil Red O-stained images of *C. elegans* cultured under control or high-glucose conditions and subsequently treated with free betanin or betanin-loaded liposomes (50 µM betanin) for 24 h, as indicated. Scale bar = 275 µm. (**D**) ImageJ-based quantification of relative lipid accumulation in *C. elegans*. Three independent experimental runs were performed, with all treatment conditions included in each run. Five individual nematodes were randomly selected from one independently treated well per condition in each run. The measurements from the five nematodes were averaged to obtain a single well-level mean, which was treated as an independent experimental observation (n = 3 independent runs per group). Quantitative data in (**B**,**D**) are presented as the mean ± standard error of the mean (SEM). Statistical significance was assessed for both (**B**,**D**) using a block ANOVA with experimental run as a blocking factor, followed by Dunnett's multiple comparisons test with the FFA-treated group as the reference for (**B**) and the high-glucose group as the reference for (**D**). * $p < 0.05$; ** $p < 0.01$.

The mean Oil Red O intensity in the Bet-CL2 group was also lower than in the free betanin and Bet-CL0 groups. Because Bet-CL2 was not compared directly with those two treatments, however, the ordering of the means is descriptive and does not establish superiority over either treatment. A significant comparison with the induction control for one formulation, and nonsignificant comparisons for others, does not itself demonstrate a difference between formulations.

A comparable response was observed in the *C. elegans* model. Lipid accumulation induced by 50 mM glucose was reduced following betanin treatment, with the lowest Oil Red O staining intensity observed in the Bet-CL2 group (Figure 5C). Quantitative analysis showed that glucose exposure increased relative Oil Red O intensity to approximately

2.3 times the control level, whereas treatment with free betanin or betanin formulations reduced the mean intensity (Figure 5D). Bet-CL2 treatment resulted in an approximately 36% reduction in relative Oil Red O intensity compared with the glucose-treated group, and this difference was statistically significant (block ANOVA, $F(4,8) = 11.08$, $p = 0.0024$, partial $\eta^2 = 0.85$; mean difference, 0.86 relative intensity units; Dunnett-adjusted $p = 0.017$; 95% simultaneous CI, 0.17 to 1.54). Thus, Bet-CL2 reduced lipid staining relative to the respective induction control in both models. The point estimates were numerically close, but the separate analyses do not test whether the treatment effects are equal or equivalent between models.

Free betanin and Bet-CL0 also yielded lower mean Oil Red O intensities than the glucose-treated group, although the lowest value was observed with Bet-CL2. However, without direct statistical evidence of differences between Bet-CL2 and free betanin or Bet-CL0, these results should be interpreted as demonstrating significant attenuation of glucose-induced lipid accumulation rather than superior efficacy over the other treatments.

The revised analysis supports a concordant direction of response in the two models: Bet-CL2 reduced Oil Red O intensity relative to the respective induction control in both. This replaces the earlier interpretation based on a significant response in *C. elegans* but not in HepG2 cells. Neither that earlier difference in significance nor the current significance in both models constitutes a direct test of a difference or equivalence between models. The results support complementary evaluation under the tested conditions, while leaving cross-model effect equivalence and a shared mechanism unresolved.

HepG2 cells provide a relatively simplified culture system comprising a single cell type, allowing hepatocyte-like responses to FFA-induced intracellular lipid accumulation to be examined under controlled conditions. In contrast, the final lipid storage phenotype in *C. elegans* may be influenced by processes occurring after oral exposure, including intestinal retention, nutrient sensing, metabolic processing, lipid transport, energy utilization, and signaling between tissues. These additional biological processes may have contributed to the organismal response to Bet-CL2.

The models differed in lipid accumulation stimulus (FFAs in HepG2 cells and glucose in *C. elegans*), betanin concentration (25 and 50 μM, respectively), and treatment schedule (co-treatment and post-induction treatment, respectively). Their percentage reductions are therefore model-specific estimates relative to different induction controls. The dual-model design permits complementary assessment under two metabolic challenges, but it does not isolate the influence of biological complexity, establish dose-matched cross-model efficacy, or demonstrate statistical equivalence of the responses.

Evaluating both models provides evidence of attenuation of lipid accumulation in a hepatocyte-like cellular system and in an intact organism under their respective exposure conditions. This complementary evidence broadens the contexts in which the formulation has been examined. It does not establish that increased carrier-associated fluorescence predicts functional efficacy or that either model predicts the response in another biological system.

The combined findings of Figures 4 and 5 support assessing carrier-associated fluorescence and functional lipid accumulation as separate endpoints. Direct measurements of betanin exposure, matched carrier controls, and comparable reference groups would be needed to quantify the relationship between delivery and function.

Considered alongside the increased cytotoxicity risk under high DOTAP exposure in Figure 4, these findings also indicate that maximizing surface charge does not necessarily yield optimal biological performance. Bet-CL2 had a lower surface charge than Bet-CL3 but exhibited high uptake-associated fluorescence without overt cellular or organismal toxicity under the conditions used for efficacy evaluation. Its lipid-lowering response was

statistically significant in both HepG2 cells and *C. elegans*. These results emphasize the need to assess physicochemical properties, biological association, safety, and functional efficacy as distinct endpoints.

Overall, Bet-CL2 lowered mean Oil Red O intensity by 33.0% relative to the FFA-treated HepG2 group and by 36.4% relative to the high-glucose *C. elegans* group; both comparisons were significant in the blocked analyses. These findings support attenuation of lipid accumulation in both models under the tested conditions. Their numerically close point estimates are descriptive and do not establish cross-model equivalence. The dual-model platform may provide a framework for complementary early-stage assessment of carrier association and functional responses.

Increasing DOTAP content altered zeta potential and encapsulation efficiency across the formulations (Figure 2B,C). In separate biological assays, the 20 mol% DOTAP formulation CL2 showed greater carrier-associated fluorescence than CL0 (Figure 4), and Bet-CL2 showed lower Oil Red O intensity than the respective induction controls (Figure 5). The approximately +31 mV value pertains to Bet-CL3, not Bet-CL2; the latter had a zeta potential of 27.88 ± 1.05 mV. These observations do not establish a continuous causal pathway from charge through betanin delivery to lipid reduction, because intracellular betanin exposure was not measured and dose-matched blank carriers were absent from the efficacy assays.

Several limitations should be considered when interpreting these findings. First, the NBD signal used to assess uptake-associated behavior originates from labeled liposomal lipids; it cannot distinguish membrane-associated carriers from internalized carriers and cannot be equated with the intracellular or tissue concentration of betanin. Direct quantification of betanin by HPLC or LC-MS, together with confocal imaging or fluorescence-quenching approaches, will be required to separate surface association from internalization. Second, dose-matched betanin-free CL0 and CL2 controls were not included alongside the efficacy experiments in Figure 5, so the contribution of the cationic carrier to lipid accumulation cannot be separated from that of betanin. The separate viability data in Figure 4C cannot resolve this efficacy-related confounding. Third, Oil Red O staining provides a relative measure of neutral lipid content, and independent indicators such as intracellular triglyceride content or molecular markers of lipid metabolism would strengthen the functional assessment. Fourth, particle size, encapsulation stability and time-dependent betanin release were not measured in the respective exposure media; betanin is sensitive to pH and oxidative conditions [9,10,14], and formulation behavior may therefore differ between cell culture medium and the *C. elegans* liquid exposure system. Fifth, the Oil Red O analyses used only four independent HepG2 runs and three *C. elegans* runs; the small sample sizes and wide confidence intervals limit precision and assessment of model assumptions. Finally, a single hepatocyte-derived cell line was used, and validation in normal, non-transformed cells and in additional cell lines remains to be performed.

4. Conclusions

In this study, we established a HepG2–*C. elegans* dual-model platform for evaluating biological interactions and lipid accumulation responses to natural compound delivery conditions at both the cellular and whole-organism levels and applied it to surface charge-modulated betanin delivery. The platform comprised an FFA-induced HepG2 steatosis model and a high-glucose-induced *C. elegans* lipid accumulation model. Within each model, formulations were compared at the same betanin-equivalent concentration (25 μM for HepG2 cells and 50 μM for *C. elegans*), with carrier-associated fluorescence, safety, and Oil Red O-based assessment of lipid accumulation serving as common evaluation endpoints. Liposomes were used as experimental tools to generate different delivery conditions by varying DOTAP content, rather than as the subject of a new encapsulation technology.

DOTAP-dependent changes in particle size, size distribution, surface charge, and betanin encapsulation efficiency were characterized, providing a physicochemical basis for interpreting the subsequent carrier-associated fluorescence signals and lipid accumulation responses. The study therefore focused on establishing an integrated evaluation framework for examining how changes in delivery conditions translate into functional responses at the cellular and whole-organism levels, extending beyond the optimization of individual formulation properties. Within this platform, HepG2 cells served as a hepatocyte-like model of lipid accumulation rather than as a cancer target.

Increasing DOTAP content from 0 to 30 mol% raised the zeta potential from -3.24 ± 0.12 to 31.09 ± 1.22 mV and the encapsulation efficiency from $35.21 \pm 1.85\%$ to $50.05 \pm 1.70\%$. NBD-CL2 produced approximately 156-fold higher cell-associated fluorescence than NBD-CL0 in HepG2 cells, and higher fluorescence was also observed descriptively in *C. elegans*. Bet-CL2 was advanced for efficacy evaluation in view of its carrier association and viability results; the high-exposure toxicity of blank CL3 motivated caution but did not establish comparative safety at the efficacy dose. In the blocked analyses, Bet-CL2 reduced Oil Red O intensity by 33.0% relative to the FFA-treated HepG2 group (Dunnett-adjusted $p = 0.0061$) and by 36.4% relative to the high-glucose *C. elegans* group (adjusted $p = 0.017$). These are separate within-model treatment effects, not evidence of statistical equivalence between models.

Analysis using NBD-labeled formulations showed that NBD-CL2 produced higher carrier-associated fluorescence than NBD-CL0 in both HepG2 cells and *C. elegans*. This observation is consistent with potentially increased cellular or organismal association or retention under DOTAP-containing delivery conditions. However, because the measured fluorescence originated from labeled lipid components, it cannot be equated with increased intracellular betanin concentrations or greater betanin delivery to tissues. Furthermore, although high exposure to blank cationic liposomes reduced HepG2 cell viability, no overt reductions in cell viability or organismal growth and survival were observed under the Bet-CL2 conditions used for efficacy evaluation. These findings highlight the importance of considering actual carrier exposure and treatment conditions alongside surface charge when assessing biological responses.

In the lipid accumulation assays, Bet-CL2 treatment significantly reduced the mean Oil Red O intensity in both models. In the FFA-induced HepG2 steatosis model, the Bet-CL2 group exhibited a significantly lower mean Oil Red O intensity than the FFA-treated group, and Bet-CL2 likewise significantly reduced lipid accumulation relative to the glucose-treated group in the high-glucose-induced *C. elegans* model. Thus, under the conditions tested, this study demonstrated attenuation of lipid accumulation by Bet-CL2 in both HepG2 cells and *C. elegans*. These findings alone, however, do not support a general conclusion that Bet-CL2 is more effective than free betanin or Bet-CL0, because those formulations were not compared directly with Bet-CL2.

The concordant direction of the responses does not establish statistical equivalence or a shared mechanism between HepG2 cells and *C. elegans*. No formal cross-model treatment-effect or equivalence test was performed. In addition to their biological organization, the models differed in the stimuli used to induce lipid accumulation—FFAs and glucose—and in their exposure conditions. The observed outcomes therefore cannot be attributed solely to differences in complexity between cellular and whole-organism systems. Accordingly, the dual-model platform is best understood as a framework for complementary interpretation of findings obtained under distinct experimental conditions, rather than as a direct comparison intended to determine which model exhibits greater efficacy. Parallel evaluation in HepG2 cells and *C. elegans* provided a basis for examining cellular responses and whole-organism lipid accumulation phenotypes together while avoiding extrapolation of findings from a single model to another level of biological organization.

Future studies should directly quantify betanin concentrations and distribution within cells and whole organisms and establish the relationship between carrier-associated fluorescence and actual betanin exposure. Controls matched for exposure level and molecular markers of lipid metabolism are also needed to examine the relationship between delivery conditions and functional responses. Furthermore, the broader applicability of the platform should be assessed using other natural compounds, delivery conditions, and additional models of metabolic disease. Validation in normal, non-transformed cells and in additional cell lines, the inclusion of dose-matched betanin-free carrier controls, and systematic measurement of encapsulation stability and betanin release under the respective exposure conditions will also be necessary before the lipid-lowering response observed here can be generalized. Overall, this study demonstrated that Bet-CL2 attenuated FFA-induced lipid accumulation in HepG2 cells and high-glucose-induced lipid accumulation in *C. elegans*, while emphasizing that neither finding should be equated with increased betanin delivery to cells or tissues. The HepG2–*C. elegans* dual-model platform established here may serve as a complementary framework for early-stage evaluation, enabling biological interactions and functional metabolic responses to natural compound delivery conditions to be examined as distinct outcomes and guiding subsequent validation.

Supplementary Materials: The following supporting information can be downloaded at https://www.mdpi.com/article/10.3390/nano16221492/s1. Additional Experimental Procedures: Physicochemical characterization of liposomes. Table S1: Composition and physicochemical properties of betanin-loaded liposomes. Figure S1: Polydispersity index (PDI) of betanin-loaded liposomes as a function of DOTAP content. Figure S2: Evaluation of the anti-steatotic efficacy of free betanin in HepG2 cells and *C. elegans*.

Author Contributions: Conceptualization, E.K., S.Y., T.-J.J. and S.M.K.; data curation, E.K.; formal analysis, E.K. and S.Y.; funding acquisition, T.-J.J. and S.M.K.; investigation, E.K., S.Y., T.-J.J. and S.M.K.; methodology, E.K. and S.Y.; project administration, T.-J.J. and S.M.K.; resources, T.-J.J. and S.M.K.; supervision, T.-J.J. and S.M.K.; validation, E.K. and S.Y.; visualization, E.K. and S.Y.; writing—original draft, E.K., T.-J.J. and S.M.K.; writing—review and editing, E.K., S.Y., T.-J.J. and S.M.K. All authors have read and agreed to the published version of the manuscript.

Funding: This work was supported by an Inha University Research Grant.

Data Availability Statement: The original contributions presented in this study are included in the article/Supplementary Materials. Further inquiries can be directed to the corresponding authors.

Conflicts of Interest: The authors declare no conflicts of interest.

References

1. World Health Organization. Obesity and overweight. Available online: https://www.who.int/news-room/fact-sheets/detail/obesity-and-overweight (accessed on 20 October 2026).
2. Chakhtoura, M.; Haber, R.; Ghezzawi, M.; Rhayem, C.; Tcheroyan, R.; Mantzoros, C.S. Pharmacotherapy of obesity: An update on the available medications and drugs under investigation. *eClinicalMedicine* **2023**, *58*, 101882. [CrossRef] [PubMed]
3. Yun, J.W. Possible anti-obesity therapeutics from nature—A review. *Phytochemistry* **2010**, *71*, 1625–1641. [CrossRef] [PubMed]
4. Kanner, J.; Harel, S.; Granit, R. Betalains—A new class of dietary cationized antioxidants. *J. Agric. Food Chem.* **2001**, *49*, 5178–5185. [CrossRef] [PubMed]
5. Hadipour, E.; Taleghani, A.; Tayarani-Najaran, N.; Tayarani-Najaran, Z. Biological effects of red beetroot and betalains: A review. *Phytother. Res.* **2020**, *34*, 1847–1867. [CrossRef] [PubMed]
6. Lee, H.S.; Choi, S.M.; Lim, S.H.; Choi, C.-I. Betanin from beetroot (*Beta vulgaris* L.) regulates lipid metabolism and promotes fat browning in 3T3-L1 adipocytes. *Pharmaceuticals* **2023**, *16*, 1727. [CrossRef] [PubMed]
7. Nirmal, N.P.; Medhe, S.; Dahal, M.; Koirala, P.; Nirmal, S.; Al-Asmari, F.; Xu, B. Betalains protect various body organs through antioxidant and anti-inflammatory pathways. *Food Sci. Hum. Wellness* **2024**, *13*, 1109–1117. [CrossRef]
8. Thong-asa, W.; Detpakdee, Y.; Srisoonthon, K. Ameliorative effects of betanin in mice with trimethyltin-induced pancreatic and hepatocytic alterations. *Sains Malays.* **2025**, *54*, 255–263. [CrossRef]

9. Amjadi, S.; Ghorbani, M.; Hamishehkar, H.; Roufegarinejad, L. Improvement in the stability of betanin by liposomal nanocarriers: Its application in gummy candy as a food model. *Food Chem.* **2018**, *256*, 156–162. [CrossRef] [PubMed]
10. Amjadi, S.; Abbasi, M.M.; Shokouhi, B.; Ghorbani, M.; Hamishehkar, H. Enhancement of therapeutic efficacy of betanin for diabetes treatment by liposomal nanocarriers. *J. Funct. Foods* **2019**, *59*, 119–128. [CrossRef]
11. Lim, S.H.; Bae, S.; Lee, H.S.; Han, H.-K.; Choi, C.-I. Effect of betanin, the major pigment of red beetroot (*Beta vulgaris* L.), on the activity of recombinant human cytochrome P450 enzymes. *Pharmaceuticals* **2023**, *16*, 1224. [CrossRef] [PubMed]
12. Liu, S.; Lian, J.; Xu, Z.; Ning, Y.; Shi, M.; Zhao, Z.; Zhang, Z. Chitosan-coated nanoliposomes for efficient delivery of betanin with enhanced stability and bioavailability. *Food Hydrocoll.* **2022**, *132*, 107871. [CrossRef]
13. Amjadi, S.; Almasi, H.; Hamishehkar, H.; Khaledabad, M.A.; Lim, L.T.; Gholizadeh, S. Gluten/chitosan nanofiber-based films activated by cationic inulin-coated betanin and carvone co-loaded nanoliposomes: Preparation and characterization. *Food Biophys.* **2024**, *19*, 243–255. [CrossRef]
14. Guan, Y.; Ning, Y.; Xu, Z.; Zhou, C.; Zhao, Z. Chondroitin sulfate and chitosan-coated liposomes as a novel delivery system for betanin: Preparation, characterization and in vitro digestion behavior. *Int. J. Biol. Macromol.* **2024**, *254*, 128001. [CrossRef] [PubMed]
15. Martínez-Rodríguez, P.; Guerrero-Rubio, M.A.; Hernández-García, S.; Henarejos-Escudero, P.; García-Carmona, F.; Gandía-Herrero, F. Characterization of betalain-loaded liposomes and its bioactive potential in vivo after ingestion. *Food Chem.* **2023**, *407*, 135180. [CrossRef] [PubMed]
16. He, H.; Lu, Y.; Qi, J.; Zhu, Q.; Chen, Z.; Wu, W. Adapting liposomes for oral drug delivery. *Acta Pharm. Sin. B* **2019**, *9*, 36–48. [CrossRef] [PubMed]
17. Miller, C.R.; Bondurant, B.; McLean, S.D.; McGovern, K.A.; O'Brien, D.F. Liposome–cell interactions in vitro: Effect of liposome surface charge on the binding and endocytosis of conventional and sterically stabilized liposomes. *Biochemistry* **1998**, *37*, 12875–12883. [CrossRef] [PubMed]
18. Sun, M.; Dang, U.J.; Yuan, Y.; Psaras, A.M.; Osipitan, O.; Brooks, T.A.; Lu, F.; Di Pasqua, A.J. Optimization of DOTAP/chol cationic lipid nanoparticles for mRNA, pDNA, and oligonucleotide delivery. *AAPS PharmSciTech* **2022**, *23*, 135. [CrossRef] [PubMed]
19. Miatmoko, A.; Asmoro, F.H.; Azhari, A.A.; Rosita, N.; Huang, C.-S. The effect of 1,2-dioleoyl-3-trimethylammonium propane (DOTAP) addition on the physical characteristics of β-ionone liposomes. *Sci. Rep.* **2023**, *13*, 4324. [CrossRef] [PubMed]
20. Kaletta, T.; Hengartner, M.O. Finding function in novel targets: *C. elegans* as a model organism. *Nat. Rev. Drug Discov.* **2006**, *5*, 387–399. [CrossRef] [PubMed]
21. Brenner, S. The genetics of *Caenorhabditis elegans*. *Genetics* **1974**, *77*, 71–94. [CrossRef] [PubMed]
22. Watts, J.L.; Ristow, M. Lipid and carbohydrate metabolism in *Caenorhabditis elegans*. *Genetics* **2017**, *207*, 413–446. [CrossRef] [PubMed]
23. O'Rourke, E.J.; Soukas, A.A.; Carr, C.E.; Ruvkun, G. *C. elegans* major fats are stored in vesicles distinct from lysosome-related organelles. *Cell Metab.* **2009**, *10*, 430–435. [CrossRef] [PubMed]
24. Zhang, S.O.; Box, A.C.; Xu, N.; Le Men, J.; Yu, J.; Guo, F.; Trimble, R.; Mak, H.Y. Genetic and dietary regulation of lipid droplet expansion in *Caenorhabditis elegans*. *Proc. Natl. Acad. Sci. USA* **2010**, *107*, 4640–4645. [CrossRef] [PubMed]
25. Markaki, M.; Tavernarakis, N. Modeling human diseases in *Caenorhabditis elegans*. *Biotechnol. J.* **2010**, *5*, 1261–1276. [CrossRef] [PubMed]
26. Leung, M.C.; Williams, P.L.; Benedetto, A.; Au, C.; Helmcke, K.J.; Aschner, M.; Meyer, J.N. *Caenorhabditis elegans*: An emerging model in biomedical and environmental toxicology. *Toxicol. Sci.* **2008**, *106*, 5–28. [CrossRef] [PubMed]
27. Gonzalez-Moragas, L.; Roig, A.; Laromaine, A. *C. elegans* as a tool for in vivo nanoparticle assessment. *Adv. Colloid Interface Sci.* **2015**, *219*, 10–26. [CrossRef] [PubMed]
28. Ashrafi, K. Obesity and the regulation of fat metabolism. In *WormBook: The Online Review of C. elegans Biology*; The *C. elegans* Research Community, Ed.; WormBook: Pasadena, CA, USA, 2007.
29. Kimura, K.D.; Tissenbaum, H.A.; Liu, Y.; Ruvkun, G. *daf-2*, an insulin receptor-like gene that regulates longevity and diapause in *Caenorhabditis elegans*. *Science* **1997**, *277*, 942–946. [CrossRef] [PubMed]
30. Subhadra, M.; Mir, D.A.; Ankita, K.; Sindunathy, M.; Kishore, H.D.; Ravichandiran, V.; Balamurugan, K. Exploring diabesity pathophysiology through proteomic analysis using *Caenorhabditis elegans*. *Front. Endocrinol.* **2024**, *15*, 1383520. [CrossRef] [PubMed]
31. Silva, A.C.; Viçozzi, G.P.; Farina, M.; Ávila, D.S. *Caenorhabditis elegans* as a model for evaluating the toxicology of inorganic nanoparticles. *J. Appl. Toxicol.* **2025**, *45*, 1124–1164. [CrossRef] [PubMed]
32. Ricchi, M.; Odoardi, M.R.; Carulli, L.; Anzivino, C.; Ballestri, S.; Pinetti, A.; Fantoni, L.I.; Marra, F.; Bertolotti, M.; Banni, S.; et al. Differential effect of oleic and palmitic acid on lipid accumulation and apoptosis in cultured hepatocytes. *J. Gastroenterol. Hepatol.* **2009**, *24*, 830–840. [CrossRef] [PubMed]

33. Fu, Y.; Li, G.; Feng, Z.; Liu, J.; Wang, X.; Wang, T.; Liu, J. Methyl cinnamate (MC) alleviates free fatty acids (FFAs) induced lipid accumulation through the AMPK pathway in HepG2 cells. *Diabetes Metab. Syndr. Obes.* **2024**, *17*, 1183–1197. [CrossRef] [PubMed]
34. Porta-de-la-Riva, M.; Fontrodona, L.; Villanueva, A.; Cerón, J. Basic *Caenorhabditis elegans* methods: Synchronization and observation. *J. Vis. Exp.* **2012**, *64*, e4019. [CrossRef] [PubMed]
35. Imamura, T.; Isozumi, N.; Higashimura, Y.; Koga, H.; Segawa, T.; Desaka, N.; Takagi, H.; Matsumoto, K.; Ohki, S.; Mori, M. Red-beet betalain pigments inhibit amyloid-β aggregation and toxicity in amyloid-β expressing *Caenorhabditis elegans*. *Plant Foods Hum. Nutr.* **2022**, *77*, 90–97. [CrossRef] [PubMed]
36. Stintzing, F.C.; Carle, R. Functional properties of anthocyanins and betalains in plants, food, and in human nutrition. *Trends Food Sci. Technol.* **2004**, *15*, 19–38. [CrossRef]
37. Rädler, J.O.; Koltover, I.; Salditt, T.; Safinya, C.R. Structure of DNA–cationic liposome complexes: DNA intercalation in multilamellar membranes in distinct interhelical packing regimes. *Science* **1997**, *275*, 810–814. [CrossRef] [PubMed]
38. Fröhlich, E. The role of surface charge in cellular uptake and cytotoxicity of medical nanoparticles. *Int. J. Nanomed.* **2012**, *7*, 5577–5591. [CrossRef] [PubMed]
39. Garcia, A.M.; Ladage, M.L.; Dumesnil, D.R.; Zaman, K.; Shulaev, V.; Azad, R.K.; Padilla, P.A. Glucose induces sensitivity to oxygen deprivation and modulates insulin/IGF-1 signaling and lipid biosynthesis in *Caenorhabditis elegans*. *Genetics* **2015**, *200*, 167–184. [CrossRef] [PubMed]
40. Alcántar-Fernández, J.; Navarro, R.E.; Salazar-Martínez, A.M.; Pérez-Andrade, M.E.; Miranda-Ríos, J. *Caenorhabditis elegans* respond to high-glucose diets through a network of stress-responsive transcription factors. *PLoS ONE* **2018**, *13*, e0199888. [CrossRef] [PubMed]
41. Wu, Z.; Li, K.; Hou, A.; Wang, Y.; Li, Z. The positive effect of *Akkermansia muciniphila* postbiotics on the glycolipid metabolism of *Caenorhabditis elegans* induced by high-glucose diet. *Nutrients* **2025**, *17*, 976. [CrossRef] [PubMed]
42. Mounkes, L.C.; Zhong, W.; Cipres-Palacin, G.; Heath, T.D.; Debs, R.J. Proteoglycans mediate cationic liposome-DNA complex-based gene delivery in vitro and in vivo. *J. Biol. Chem.* **1998**, *273*, 26164–26170. [CrossRef] [PubMed]

Disclaimer/Publisher's Note: The statements, opinions and data contained in all publications are solely those of the individual author(s) and contributor(s) and not of MDPI and/or the editor(s). MDPI and/or the editor(s) disclaim responsibility for any injury to people or property resulting from any ideas, methods, instructions or products referred to in the content.